CHEMICAL ENGINEERING TRANSACTIONS
VOL. 93, 2022
A publication of AIDIC
The Italian Association of Chemical Engineering
Online at www.cetjournal.it
Guest Editors: Marco Bravi, Alberto Brucato, Antonio Marzocchella

ISBN 978-88-95608-91-4; **ISSN** 2283-9216
DOI: 10.3303/CET2293022

Numerical Simulations of Mass Transfer Prediction in a Photobioreactor

Miroslav Rebej*, Jiří Vondál, Tomáš Juřena, Vladimír Brummer, Zdeněk Jegla, Martin Naď

Institute of Process Engineering, Brno University of Technology, Technická 2896/2, 61669, Brno, Česká republika
rebej@fme.vutbr.cz

The paper deals with the possibility of using flue gas as a nutrient source for microalgae cultivation in a bubble column photobioreactor. The experiments performed on a vertical tubular photobioreactor determined the concentrations of the flue gas species that pass from the flue gas into the cultivation medium. The flue gas used for experiments was a gas mixture of different pollutants, e.g. SO_x, NO_x, or CO_2, with a composition typical for waste-to-energy facilities. The paper is supplementary to the laboratory experiments. The objective of the multiphase CFD analysis is to develop the numerical model for mass transfer predictions in photobioreactors. The model employs the Henry's law for interphase equilibrium and the penetration model for the mass transfer coefficient.

1. Introduction

Microalgae cultivation may be one of the possible ways to meet environmental challenges. Cultivation of microalgae creates biomass that can be processed into other products such as proteins, lipids, carbohydrates, vitamins or pigments that can be turned into biofuels or other substances with potential use in cosmetics, agriculture or medicine (Vassilev and Vassileva, 2016). The microalgae species diversity allows their use in various areas as each specie has different requirements for living conditions.
Microalgae can effectively remove some substances from waste streams. Examples of these substances are gaseous pollutants, e.g. CO_2, NO_x, SO_x, heavy metals or other substances like phosphates, sodium, magnesium or calcium. Ideally, appropriate cultivation of microalgae could, therefore, capture various pollutants that would negatively affect the environment and, at the same time, transform waste products into valuable raw materials and biomass production. Waste products can consequently become a cheap source of nutrients for microalgae that could be used to produce other products. The use of waste products may subsequently reduce the impact of human activities on the environment and obtain a sustainable way of dealing with them. However, it is necessary to maximize photobioreactor efficiency for such processes to be economical and feasible.
The mass transfer in the gas-liquid environment often becomes the rate-limiting step for the overall reaction because of the low solubility of most gases (Kraakman et al., 2011). As a result, a photobioreactor for gas treatment can reach the mass-transfer-limited conditions. The purpose of the presented work is to develop a CFD model that is supplementary to mass transfer experiments in photobioreactors under CO_2-enriched conditions.

2. Experimental photobioreactor

All experiments described in this paper were performed on the pilot experimental photobioreactor. The photobioreactor is a bubble-column type with three vertical tubes. The photobioreactor schematic is in Figure 1. The cultivation medium was aerated from the bottom of the tubes through the perforated inlet membrane. The aeration gas mixture was pumped from the gas tanks, with the oxygen being stored in one tank and the mixture of flue gases in the other tank.

Paper Received: 20 December 2021; Revised: 15 March 2022; Accepted: 19 April 2022
Please cite this article as: Rebej M., Vondál J., Jurena T., Brummer V., Jegla Z., Nad M., 2022, Numerical Simulations of Mass Transfer Prediction in a Photobioreactor, Chemical Engineering Transactions, 93, 127-132 DOI:10.3303/CET2293022

This disposition prevented the oxidation of flue gases and allowed the preparation of the desired gas mixture for the aeration. The aeration gas mixture was then pumped into the buffer tank and fed into the reactor's tubes. The aeration gas that had passed through the cultivation medium was then collected and returned to the buffer tank. However, before entering the buffer tank, the gas composition was analysed.
In addition to that, the photobioreactor loop is equipped with a peristaltic pump to extract any produced biomass.

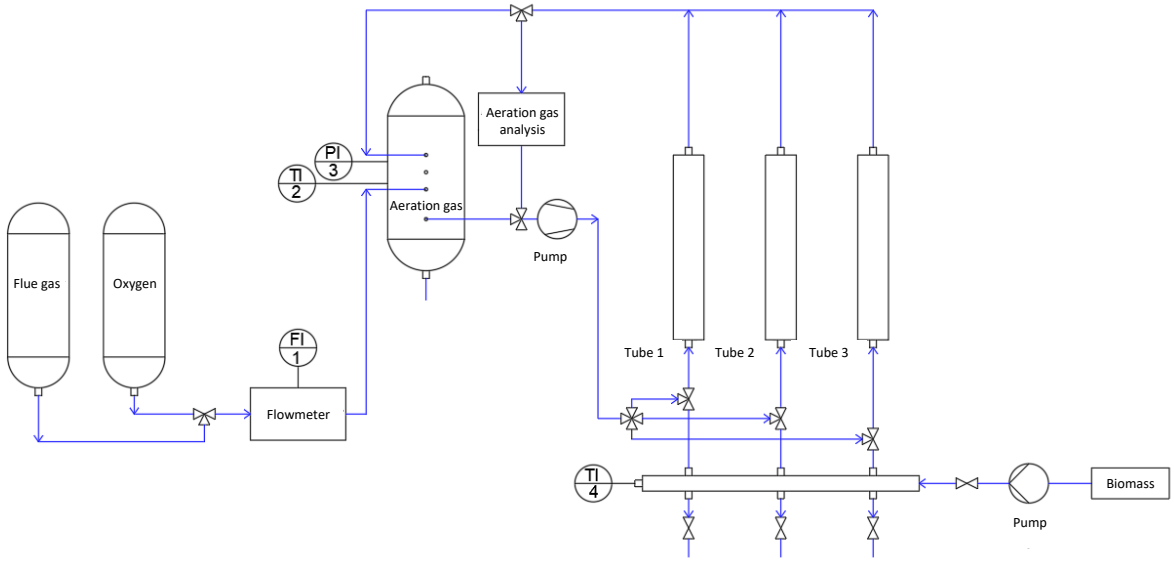

Figure 1 Schematic of the pilot experimental photobioreactor

2.1 Aeration gas mixture

The reactor was filled with 4.34 L of water (1.447 L in each tube), and the experiments took place at an ambient temperature of 22°C. In total, 105 L of the aeration gas was fed to the reactor from storage tanks with composition presented in Table 1. To measure real-time changes in the composition of the aeration gas after passing through the cultivation medium, the ABB EL3020 continuous flue gas analyser was used. The experiment took 1 h 40 min with the constant airflow rate of 2 L/min at 165 mbar.

Table 1 Aeration gas composition

Substance	Amount	
SO_2	50	mg m_N^{-3}
CO	50	mg m_N^{-3}
NO	200	mg m_N^{-3}
O_2	9	$\%_{vol.}$
CO_2	10	$\%_{vol.}$
N_2	81	$\%_{vol.}$

3. Numerical model

3.1 Geometry and computational mesh

To simplify the numerical model only one tube with a height reduced to 1 m was modelled. The bottom of the modelled domain was set above the perforated inlet membrane as bubbles were found to occupy the tube cross-sectional area almost immediately. Therefore, the model geometry follows the plain inner volume of the tube with a rectangular cross-section of dimensions 44x20 mm and rounded corners with 10 mm radius. The computational mesh was made in the ANSYS SpaceClaim 2021 R2 (ANSYS Inc., 2021) with 39,288 polyhedral cells. Regarding the mesh quality, the minimum orthogonal quality is 0.5, max. cell size is 3.77 mm. Furthermore, the geometry was divided into two cell zones, the inlet zone and the domain zone.

The inlet cell zone grows from the bottom surface up to the height of one cell, and the domain cell zone fills the rest of the tube volume. This modification allowed to neglect the geometry of the perforated inlet membrane and to model the inlet boundary condition as a mass source term. The top surface was defined with the degassing boundary condition, i.e. a free-slip wall for the liquid phase and an outlet for the gaseous phase. Other walls were treated as the no-slip wall for all phases.

3.2 Numerical model

The numerical model is based on the Eulerian-Eulerian multiphase framework in the ANSYS Fluent 2021 R2 (ANSYS Inc., 2021). The framework uses two phases, the primary phase with liquid water and liquid CO_2, and the secondary phase with the aeration gas. However, to further simplify the numerical model, the modelled composition of the aeration gas neglected the three least frequent components. Individual mass diffusion coefficients are listed in Table 2.

Table 2 Diffusion coefficients (Cussler, 2009)

Species pair	Diffusion coefficient, cm^2/sec
$CO_2 – O_2$ (g)	0.156
$CO_2 – N_2$ (g)	0.165
$N_2 – O_2$ (g)	0.220
$H_2O – CO_2$ (l)	1.92e-5

The uniform bubbly flow had developed shortly after the air injection, see Figure 2, and the equivalent bubble diameter was found with the image processing of the projected bubble area. The mean bubble diameter was determined to be 4.5 mm and it was considered as the diameter of a sphere with the same projected area as the measured bubble. Therefore, in the numerical model, the secondary phase was modelled with the formulation of spherical bubbles with the mean diameter of 4.5 mm. The interphase interaction force only included the Ishii-Zuber drag model.

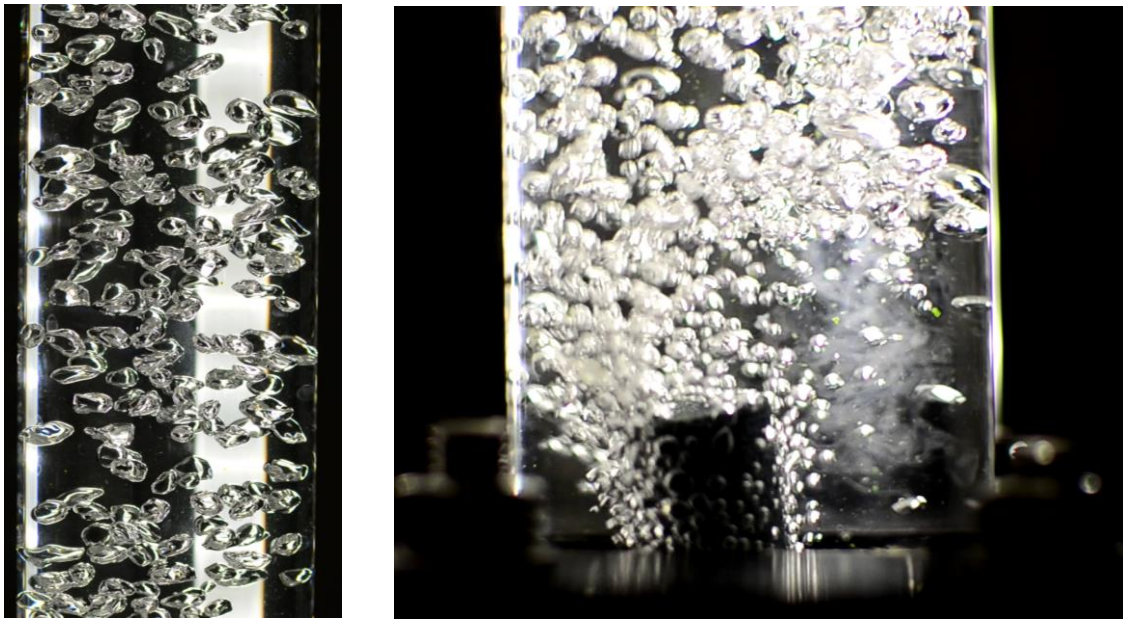

Figure 2 Bubble size and distribution: mid-height (left) and inlet (right)

The interphase equilibrium model for the interphase species mass transfer employed the Henry's law formulation. The molar concentration was 3,030,300 (Pa m^3)/kmol (Sander, 2015). Next, the penetration model (Higbie, 1935) was used to determine the mass transfer coefficient. The penetration model was found to be suitable for weakly turbulent flows (Gao et al., 2015), Eq (1).

$$k_L = \sqrt{\frac{4D_L u_{slip}}{\pi d_B}} \quad (1)$$

where the mass-transfer-coefficient is based on the phase diffusivity, D_L, slip velocity, u_{slip}, and the characteristic length, d_B, e.g. bubble diameter. This yields the mass transfer coefficient of 8.5 10^{-5} m/s. The respective rising velocity in water for bubbles 4.5 mm large in diameter is around 0.35 m/s. Therefore, it can be concluded that the hydrodynamic phenomenon defines the time scale of the numerical model. Considering 4 mm cell size, the time step size 0.005 s yields the Courant number of 0.5.
Equations for momentum, continuity, volume fraction, energy and interphase species mass transfer were solved with the pressure-based phase-coupled algorithm. The second-order spatial discretization was employed for momentum equations and PRESTO! for the pressure discretization. The numerical model was initialized with the domain filled with quiescent liquid water only.

4. Results

The duration of the experiment and numerical analysis took 30 min of flow time. Figure 3 shows the CO_2 volume fraction in the aeration gas at the outlet of the tube. At the beginning of the aeration, the water did not contain any CO_2, resulting in the highest concentration gradient yielding the max mass transfer rate of 2 g/(m^3 s). Considering the superficial velocity of 13.3 mm/s, it can be assumed that the mass transfer rate was the dominant phenomenon at the beginning of aeration, rendering the drop below 8 $\%_{vol.}$ CO_2. In the case of the laboratory experiment, the combination with a pressure drop in the aeration gas loop could have caused an even lower concentration drop. However, the time to reach the saturated state is approximately 15 min in the CFD prediction and laboratory experiment. After this time, the flow can be considered developed and stabilized. Figure 2 shows that bubbles in the inlet region grow in their size until they are uniform in their size and shape. Considering the constant bubble diameter in the Higbie's formulation of the mass transfer coefficient, the mass transfer rate might be under-predicted for the beginning of the simulation as larger bubbles provide less interfacial area and experience more drag, i.e. move with lower velocity. Therefore, smaller bubbles in combination with the largest concentration gradient between water and CO_2-rich gas could yield a higher mass transfer rate (Geng Shigang and Meng Weidong, 2018) rendering a lower drop in the first 5 minutes of the flow in Figure 3.

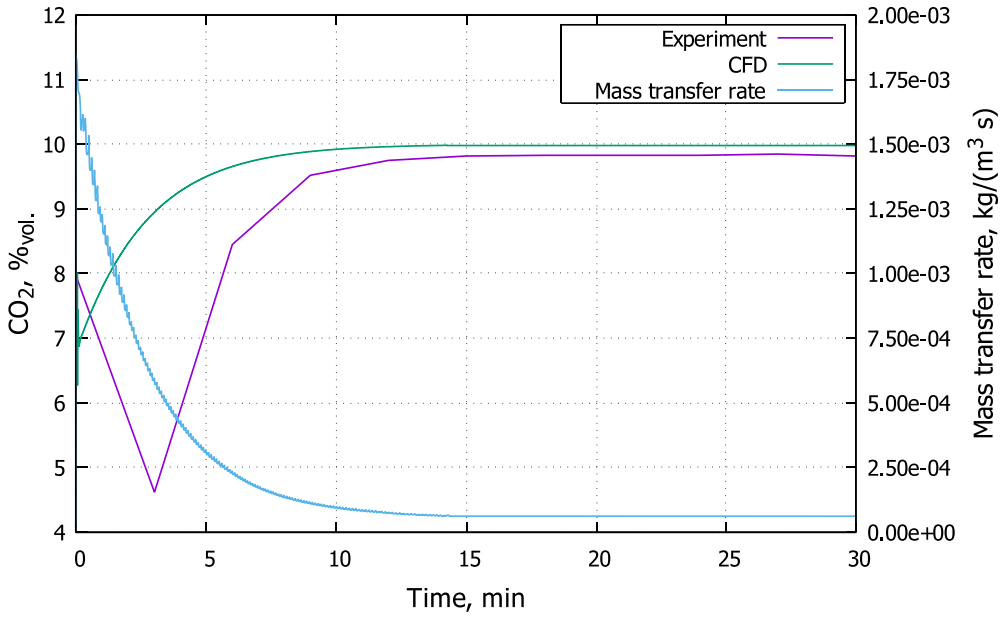

Figure 3 Volume fraction of CO_2 and mass transfer rate in the aeration gas

Due to the relatively small cross-sectional area and high air velocity, the concentration of CO_2 in both phases is uniform. As a result of a uniform concentration gradient, the mass transfer rate is uniform as well, see Figure 4. A noticeable difference in the region close to the inlet is observable only in the first 6 minutes.

After this point, it is diminished and the liquid phase saturation becomes the limiting factor and the mass transfer is not affected by the concentration gradient to such extent. After 30 min, the CO_2 concentration in the liquid phase is between 0.160 to 0.165 kg/m^3 and the mass transfer rate is in the order of 2.0 10^{-5} kg/(m^3 s).

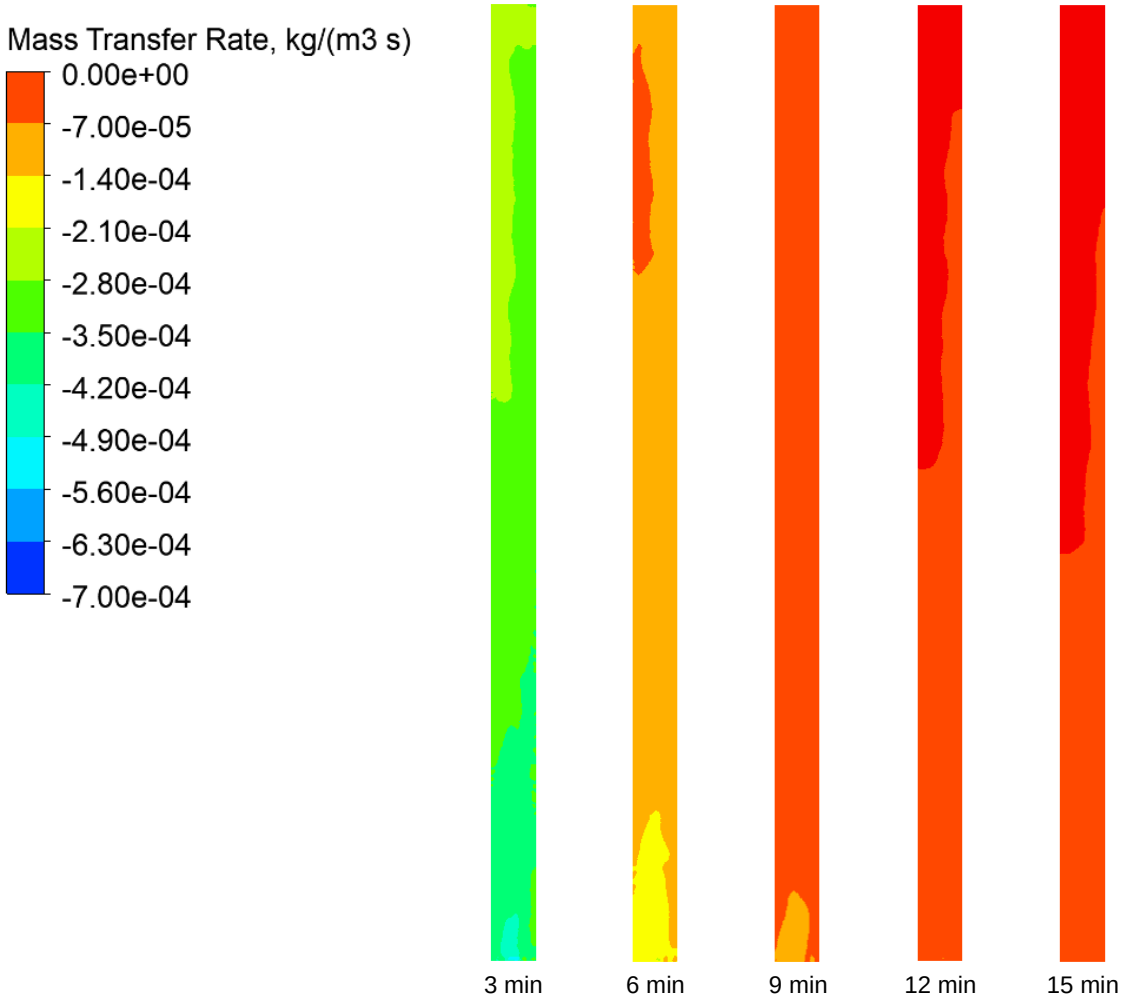

Figure 4 Contours of instanteneuos mass transfer rate at 3 minute intervals. Displayed on the mid-plane.

5. Conclusions

The following conclusions can be drawn from the study:

- Time evolution of CO_2 concentration in flue gas shows a good qualitative agreement of the CFD model with experimental data.
- The time to reach saturated state is predicted correctly by the CFD model.
- Local minimum during the initial drop of CO_2 in the gas phase is overestimated. The difference can be caused by the underestimated mass transfer in the bottom part, where turbulence is the most intensive.
- Predicted mass transfer rate is sensitive to the estimate of the average bubble diameter and slip velocity of the bubbles through the penetration model and surface-to-volume ratio of the bubble.
- The concentration of CO_2 in saturated liquid mixture is slightly underestimated, which can be caused by the simplified (binary) model.
- The study reveals that the CO_2 concentration field is homogeneous in the entire tube volume.
- The well-mixed reactor condition supports the sampling methodology during the experiments so that the samples taken from the bottom of the reactor are representative of its volume.
- The model may serve to supplement the real experiment in a preliminary analysis of mass transfer in the reactor. It offers relatively short turnaround times comparable to experiments.

Acknowledgments

This research was supported by the EU project Strategic Partnership for Environmental Technologies and Energy Production, funded as project No. CZ.02.1.01/0.0/0.0/16_026/0008413 by Czech Republic Operational Programme Research, Development and Education, Priority Axis 1: Strengthening capacity for high-quality research.
Miroslav Rebej is the Brno Ph.D. Talent Scholarship Holder – Funded by the Brno City Municipality.

References

ANSYS Inc., 2021. ANSYS Fluent Theory Guide, Release 2021 R2. ANSYS Inc., Canonsburg, PA, USA.

Cussler, E.L., 2009. Diffusion: Mass Transfer in Fluid Systems, Cambridge Series in Chemical Engineering. Cambridge University Press.

Gao, X., Kong, B., Ramezani, M., Olsen, M.G., Vigil, R.D., 2015. An adaptive model for gas-liquid mass transfer in a Taylor vortex reactor. International Journal of Heat and Mass Transfer 91, 433–445. https://doi.org/10.1016/j.ijheatmasstransfer.2015.07.125

Geng Shigang, Meng Weidong, 2018. Chemical absorption and mass transfer of greenhouse gas carbon dioxide. Chemical Engineering Transactions 71, 1–6. https://doi.org/10.3303/CET1871001

Higbie, R., 1935. The rate of absorption of a pure gas into still liquid during short periods of exposure. Transactions of the American Institute of Chemical Engineers 31, 365–377.

Kraakman, N.J.R., Rocha-Rios, J., van Loosdrecht, M.C.M., 2011. Review of mass transfer aspects for biological gas treatment. Appl Microbiol Biotechnol 91, 873–886. https://doi.org/10.1007/s00253-011-3365-5

Sander, R., 2015. Compilation of Henry's law constants (version 4.0) for water as solvent. Atmospheric Chemistry & Physics 15, 4399–4981. https://doi.org/10.5194/acp-15-4399-2015

Vassilev, S.V., Vassileva, C.G., 2016. Composition, properties and challenges of algae biomass for biofuel application: An overview. Fuel 181, 1–33. https://doi.org/10.1016/j.fuel.2016.04.106